NEOPLASIA
www.neoplasia.com

Volume 22 Number 5 May 2020 pp. 220–230

MKL1/miR-5100/CAAP1 loop regulates autophagy and apoptosis in gastric cancer cells

Hui-Min Zhang [1]; Hui Li [1]; Gen-Xin Wang [1]; Jun Wang [1]; Yuan Xiang [1]; You Huang; Chao Shen; Zhou-Tong Dai; Jia-Peng Li; Tong-Cun Zhang *; Xing-Hua Liao *

Institute of Biology and Medicine, College of Life and Health Sciences, Wuhan University of Science and Technology, 430000, PR China

Abstract

Purpose: miR-5100 participates in the proliferation of lung cancer and pancreatic cancer cells, and participates in the differentiation of osteoblasts. However, the regulation of gastric cancer cells in gastric cancer cells remains unclear.
Experimental design: The blood of patients was collected to detect the expression level of miR-5100, and the apoptosis and autophagy levels of cells were detected using western blot, flow cytometry, and confocal. At the same time, in vitro tumor formation experiments in nude mice were used to verify the results of in vitro experiments.
Results: The expression of miR-5100 is related to the prognosis of gastric cancer, miR-5100 can enhance the apoptosis level of gastric cancer cells and inhibit the occurrence of autophagy by targeting CAAP1. MKL1 can inhibit the apoptosis of gastric cancer cells and promote the occurrence of autophagy by targeting CAAP1. At the same time, MKL1 can also increase the expression of miR-5100.
Conclusions: Our research reveals the mechanism by which the MKL1/miR-5100/CAAP1 loop regulates apoptosis and autophagy levels in gastric cancer cells, and miR-5100 is expected to become a new potential target for gastric cancer treatment.

Neoplasia (2020) 22 220–230

Keywords: MKL1, miR-5100, CAAP1, Autophagy, Apoptosis, Gastric cancer

Introduction

Cancers have long been great threats to human society, causing both economic burdens and patient sufferings. Among the various types of cancers, gastric cancer (GC) belongs to the most commonly diagnosed ones [1]. according to the data of the World Health Organization, GC is the fifth most common cancer and the third leading cause of cancer mortality in worldwide [2,3]. Although a series of research progress has been made in diagnosis and treatment of GC, the 5-year survival rate of GC is no more than 25 percent [4]. Invasion, metastasis and recurrence are the common cause for death rate of this disease. Therefore, it's necessary to study the molecular event underlying progression and to find the novel therapeutic target of gastric cancer.

miRNAs are short non-coding RNAs that have become post-transcriptional regulators of various physiological processes involved in cells, such as cell growth, movement, invasion, autophagy, apoptosis, and stress response [5–7]. The main mechanisms by which miRNAs regulate target genes include induction of mRNA degradation and inhibition of mRNA translation by binding to partially complementary sequences in the 3′ untranslated region [8,9]. Discovering the molecular regulatory pathways by which miRNAs control gastric cancer contributes to a better understanding of cancer biology and new targeting strategies for the future treatment of gastric cancer. Existing literature has proved that miR-5100 is highly expressed in lung cancer cells and can affect the formation of tumors by affecting the autophagy of cells [10,11]. In our previous study, we demonstrated that miR-5100 is over-expressed miRNA in gastric cancer, but the function of miR-5100 has not been reported yet. In this study, we report that miR-5100 modulates tumor growth in lung cancer and identify CAAP1 as a direct target of miR-5100. Our data reveal a novel regulation circuit for gastric cancer cell growth and demonstrate that miR-5100 serves as a potential target for gastric cancer therapy.

C9orf82 protein, or conserved anti-apoptotic protein 1 or caspase activity and apoptosis inhibitor 1 (CAAP1) has been implicated as a negative regulator of the intrinsic apoptosis pathway by modulating caspase expression and activity. CAAP1 was proposed to modulate a Caspase-10

* Corresponding authors at: Institute of Biology and Medicine, College of Life and Health Sciences, Wuhan University of Science and Technology, Hubei 430081, PR China. Fax: +27 6889 3590.
e-mail addresses: 1972674907@qq.com (G.-X. Wang), zhangtongcun@wust.edu.cn (T.-C. Zhang), xinghualiao@wust.edu.cn (X.-H. Liao).
[1] These authors contributed equally to the paper.

https://doi.org/10.1016/j.neo.2020.03.001

dependent mitochondrial Caspase-3/9 feedback amplification loop [12]. In recent years, CAAP1 has been gradually valued in tumor cells and started to be a new target in tumor therapy.

As a family of myocardin-related transcription factors (MRTF), megakaryoblastic leukemia 1 (MKL1) is widely expressed in many tissues [13–15] and functions as a co-activator serum response factor (SRF), which plays an important role in the control of active or contractive cell function, especially in cancer metastasis, vascular smooth muscle cell and cardiac muscle cell differentiation [16,17]. Recent studies have shown that mkl1 may also be involved in cell proliferation in gastric cancer cells [18,19]. At the same time the actin cytoskeleton, and the main transcription factor complex controlling its abundance, MKL1/SRF, limits cell fate reprogramming by regulating global chromatin accessibility [20,21]. Therefore, MKL1 is also important for apoptosis and autophagy in gastric cancer cells.

Materials and methods

Cell lines

Human gastric cancer cell lines MGC80-3, AGS, SGC-7901 were bought from American Type Culture Collection (ATCC, Manassas, VA) MGC80-3, SGC-7901 cultured in RPMI 1640 medium (GIBCO) and AGS cultured in D-MEM/F-12 (GIBCO) supplemented 10% fetal bovine serum (FBS; Biological Industries) in the incubator with a humidified atmosphere (5% CO_2, 37 °C).

Plasmids

The coding region sequences of MKL1 and CAAP1 genes were amplified by PCR using the cDNA of gastric cancer cells as the template (MKL1:forward: 5′-ATGGCCCAATGGAATCAGCTACAGC-3′,reverse:5′-TCACATGGGGGAGGTAGCGCACTCCGA-3′;CAAP1:forward: 5′-AGAGGGATCATGACGGGGAAAAAGT-3′,reverse:5′-TACCTAG GCTGGCTTTTTTATATCA-3′) and inserted into mammalian expression vector pcDNA3.1 (Invitrogen, USA), respectively. The promoter sequences of CAAP1 (-465+45) and miR5100 (-516-0) were amplified by PCR (WT-CAAP1-Luc forward: 5′-TGTCCATGTCAGACTC TACGCAAGA-3′ WT-CAAP1-Luc reverse: 5′-ATCGGAGGAAAGTC CGCTGTCTCTG-3′; WT-miR5100-Luc forward: 5′-CTGTTCTTGG TGGTCAGGTG-3′, WT-miR5100-Luc reverse: 5′-CTGTTTCTGAA GGTGATGGAG-3′) and inserted into the luciferase vector pGL3-Promoter (Addgene, USA) using mammalian genome as template. MUT-CAAP1-Luc (The binding site of MKL1 was mutated) forward: 5′-GCAAGAAATATTTAATTTGCCCAGGTGATGAGGAAAATGA GATGGAACA-3′, reverse: 5′-GGGCAAATTAAATATTTCTTGCGTA GAGTCTGACATGGACAAGTAGAGCTT-3′; MUT-miR5100-Luc (The binding site of MKL1 was mutated) forward: 5′-GGCCAGGG TAATTTTTAATACTGGAACCTCTCCAAGCTCACCAGCACTC-3′ , reverse: 5′-GGTTCCAGTATTAAAAATTACCCTGGCCCCGAGAG GCCACCTGA-3′; The CAAP1 3′-UTR sequence was amplified by PCR (WT-pmir-CAAP1 forward: 5′-GTATTTAACTTGATTTT GAATTTTAG-3′,WT-pmir-CAAP1 reverse: 5′-TTCATGAAGGTGGA GACTTTA-3′) and inserted into dual-luciferase miRNA target expression vector pmirGLO (Invitrogen, USA) using the mammalian genome as the template; as for MUT-pmir-CAAP1 (The binding site of miR5100 was mutated) Since three sites on CAAP1 3′UTR bind to miR-5100, we made two mutations, using the following primers: MUT-pmir-CAAP1-1 forward: 5′-TCATTCTG CACGTAGC GACTTTTGATACTTTTTCA AAAGCAAAAT-3′, reverse: 5′-CAAAAGTCGCTACGTGCAGAATGA TAGCATTTTATTATTTCTGAT-3′; MUT-pmir-CAAP1-2 forward: 5′-TTGCTTAAAACTGCAGTGTGCTATAATTCCATGAATCAGAA ATAA-3′, reverse: 5′-TATAGCACACTGCAGTTTTAAGCAACTA CATCAGATAAAATCCTA-3′.

Transfection

Negative control mimic (NC mimic), miR-5100 mimic (mimic), Negative control inhibitor (NC inhibitor), miR-5100 inhibitor (inhibitor) Negative control siRNA (si-NC), siRNA-MKL1 (si-MKL1), siRNA-CAAP1 (si-CAAP1) were purchased from RIBOBIO biological. All plasmids were extracted with EndoFree Plasmid Midi Kit (CWBIO), all fragments and plasmids were transfected with lipofectamine 3000 (Invitrogen, USA) according to the manufacturer's instructions.

RT-PCR and qRT-PCR

RNA was extracted using ultrapure RNA Kit (CWBIO), 1 ug RNA was reverse-transcribed into cDAN using PrimeScript RT reagent Kit With gDNA Eraser (Takara), and Hieff qRT-PCR SYBR Green Master Mix was used for qRT-PCR (Yeasen). The primers involved are as follows: GAPDH: forward: 5′-GGAGCGAGATCCCTCCAAAAT-3′, reverse: 5′-GGCTGTTGTCATACTTCTCATGG-3′; CAAP1: forward: 5′-AGTA CCGACTCTTCCAGCGTCT-3′, reverse: 5′-CAAGGTCACTGTGCT CTGCCAA-3′.

Luciferase assay

The cells were seeded at 2×10^4 cells/well in 24-well cell culture plates, the cells were harvested after transfection for 24 h, then lysed on ice for 30 min with 1 × Passive Lysis Buffer (Promega). After centrifugation, 10 μL of the supernatant was added to measure the fluorescence value by adding 100 μL of Luciferase Assay Buffer (Promega). Take the same volume of supernatant and measure the protein concentration with the Enhanced BCA Protein Assay Kit to finally calculate the fluorescence value per unit protein concentration.

Western blotting

The cells were lysed with RIPA Lysis Buffer (Beyotime) and the proteins were quantified with the Enhanced BCA Protein Assay Kit (Beyotime), 40ug of protein per protein lane, then, the protein was transferred to the polyvinylidene fluoride (PVDF) Membrane (Millipore), sealed with 5% skimmed milk powder for 1 h, and incubated overnight with primary antibody at 4 °C, The antibodies used are as follows: Anti-GAPDH (1:2 000, Abclonal), Anti-CAAP1 (1:500, Sigma), Anti-MKL1 (1:1 500, Cell Signaling Technology/CST), Anti-Caspase3 (1:1 500, CST), Anti-LC3B (1:1 500, CST), Incubate secondary antibodies conjugated with named horseradish peroxidase–labeled (HRP) (Santa Cruz) at room temperature for 1 h, Samples were detected by Western fluorescence assay BeyoECL Plus (Beyotime).

Chromatin immunoprecipitation assay

Follow the instructions of the SimpleChIP® Enzymatic Chromatin IP Kit (Agarose Beads) strictly with a 37% formaldehyde solution for cross-linking. Rinse the cells twice with pre-chilled PBS and collect the cells. Then centrifuge the cells for 10 min at 1 500 rpm at 4 °C and discard Supernatant. The resulting cells were collected for nuclear processing and chromatin shearing. We digested the sample DNA into 150–900 bp fragments using micrococcal nuclease, centrifuged at 13 000 rpm for 3 min at 4 °C to precipitate the nucleus, and then sonicated the nucleus, and then kept it at 1 000 rpm for 10 min at 4 °C to retain Supernatant; the samples were divided into three groups during chromatin

immunoprecipitation. Target protein antibody, IgG antibody, and no antibody were added to each group at 4 °C overnight. ChIP-grade protein G agarose beads were added to each group and incubated; the beads were eluted and cross-linked, and the DNA was purified by a spin column for PCR. The results were analyzed by 2% agarose gel electrophoresis.

Autophagy assay

CYTO-ID® Autophagy detection kit was adopted to detect autophagy. The cells were cultured on 14 × 14 mm cell slides and the culture medium was carefully removed after transfection 48 h, when the cells reached a confluence level of 50–70%. Distribute 100 μL of Dual Detection Reagent to cover monolayer cells, prevent the sample light and incubation for 30 min at 37 °C, carefully wash the cells with 100 μL of 1 × Assay Buffer, Remove excess buffer and place coverslip upside down on microscope slide, Analyze the stained cells by confocal microscopy, Use a standard FITC filter set for imaging the autophagic signal, image the nuclear signal using a DAPI filter set.

Flow cytometry

The apoptosis assay was performed using the Annexin V-FITC/PI Apoptosis Detection Kit (Meilunbio). The cells after 48 h of transfection were trypsinized without EDTA, and then collected by centrifugation at 500–1 000*g* and washed twice with pre-cooled PBS. 1 × Binding buffer After resuspending the cells, 5 μL Annexin V-FITC and 5 μL PI were added to 100 μL of cell suspension and gently mixed, and incubated for 15 min at room temperature to avoid light. Before using the flow cytometry (BD) to detect cells, add 400 μL of 1 × Binding buffer working solution to each tube and mix well after staining and incubation. Experimental results using Flowjo software for analysis and mapping.

Hematoxylin-Eosin staining

Tumor tissue from nude mice was sent to Servicebio Biotech for paraffin-embedded sectioning. Hematoxylin-Eosin/HE Staining Kit (Solarbio) is used for hematoxylin-eosin staining. Paraffin section dewaxing, hematoxylin dyeing, differentiation, eosin staining, dehydration, transparent, sealing, neutral gum sealing, microscopic observation, all the above operations in strict accordance with the manufacturer's instructions.

Immunohistochemistry experiment

We used the Streptavidin-alkaline phosphatase (SABC--AP) immunohistochemical staining kit (BOSTER Biological) for immunohistochemistry experiment. Briefly, Paraffin section dewaxing, heated antigen retrieval, 5% BSA blocking solution overnight at 4 °C, incubation at 37 °C for 2 h, then biotinylated goat anti-rabbit IgG 37 °C for 30 min, SABC-AP Incubate at 37 °C for 30 min. After BCIP/NBT color development, the nuclear solid red is lightly counterstained, then neutral resin sealing, observe under the microscope. All the above steps are strictly in accordance with the manufacturer's instructions.

Human tumor xenograft model

The animal experiment program has obtained the consent of the Experimental Animal Center of Wuhan University of Science and Technology and the Committee of Experimental Animal Ethics Review. BALB/c-nu (nude) mice were obtained from Beijing Vital River (Charles River Laboratories). Four-week-old nude mice were randomly divided into 4 groups, and 1×10^7 AGS cell lines stably overexpressing miR-5100 and a control group were injected subcutaneously separately, so that we got four groups: two groups were injected with AGS cell lines stably overexpressing miR-5100 (miR-5100-plko.1), two groups of control groups (plko.1), 14 days later, a group of miR-5100- plko.1 and plko.1 groups were administered with paclitaxel twice a week (Named miR-5100-plko.1+Taxol, plko.1+Taxol). All nude mice were euthanized after 35 days. Carefully remove the tumor tissue from the nude carcass to count the volume and weight of the tumor.

Clinical sample

We obtained 30 clinical samples of gastric cancer from the Affiliated Hospital of Huazhong University of Science and Technology. The samples were collected from September 2018 to the end of September 2019. All the clinical samples collected were obtained from the informed consent of the patients. The research protocol complied with the ethical guidelines of the Helsinki Declaration (1975) and was approved by the Medical Ethics Committee of Wuhan University of Science and Technology Approved. At least two pathologists confirmed the diagnosis of GC pathology.

Statistical analysis

All the experiments in the article were completed three times independently. The values were presented as the mean þ standard deviation. Two-sided P values <0.05were considered statistically significant.

Results

miR-5100 promotes apoptosis and inhibits autophagy of gastric cancer cells

Initially, we collected gastric cancer tissues and normal tissues from 30 gastric cancer patients, extracted miRNA from the tissues, and detected miR-5100 expression levels by qRT-PCR. It was found that the expression level of miR-5100 in gastric cancer tissue was lower than that in normal gastric tissue (Fig. S1A). Next, we extracted total miRNA from GES1, MGC80-3, AGS and SGC7901 cell lines, and detected the expression level of miR-5100 by qRT-PCR. The results showed that compared with GES1 cell lines, MGC80-3, AGS and SGC790 cell lines MiR-5100 has lower expression levels. In summary, we have initially concluded that miR-5100 expression is low in gastric cancer tissues and gastric cancer cell lines.

In order to study whether miR-5100 has an effect on the apoptosis of gastric cancer cells, miR-5100 inhibitors or inhibitor controls were transfected into MGC80-3 cell line, and Western blot was used to detect the expression of Caspase3 and Cleaved-Caspase3 (Fig. 1A), Statistical analysis showed that the expression level of Cleaved-Caspase3 decreased ($P < 0.05$) (Fig. 1B); changes in apoptosis levels were detected by flow cytometry (Fig. 1C), and statistical results showed that the level of apoptosis was decreased ($P < 0.05$) (Fig. 1D). In the AGS cell line, we found that miR-5100 minic promotes Cleaved-Caspase3 protein expression ($P < 0.05$) (Fig. 1E, F) and promotes apoptosis (Fig. 1G, H). These results indicate that miR-5100 can promote the apoptosis of gastric cancer cells. In order to investigate whether miR-5100 affects gastric cancer cell autophagy, miR-5100 inhibitors or controls were transfected into MGC80-3 cells. The level of LC3B expression in the cells changed (Fig. 1I), and the ratio of protein LC3BII/I was up-regulated. ($P < 0.05$) (Fig. 1J), the autophagosome content of the cells was increased under the confocal microscope (Fig. 1K). In the AGS cell line, miR-5100 minic promotes a decrease in the proportion of proteins that promote LC3BII/I (Fig. 1L, M), and autophagosome content of the cells decreases under confocal

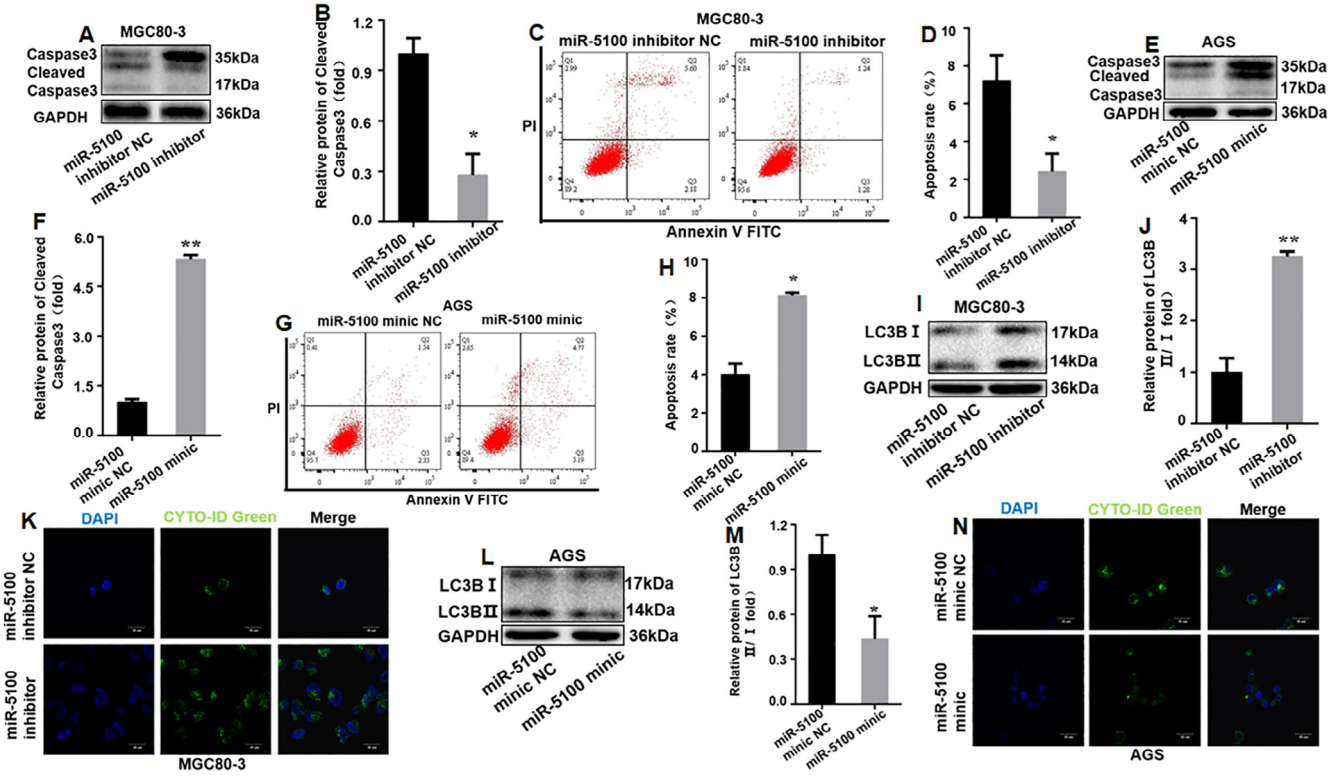

Fig. 1. miR-5100 promotes apoptosis and autophagy in gastric cancer cells. miR-5100 inhibitor or miR-5100 inhibitor NC (control group) transfected into MGC80-3 cells. (A-B): The expression of caspase3 and cleaved-caspase3 protein was detected by western blot, and the cleaved-caspase3 protein was statistically analyzed, $P < 0.05$; (C-D): Cell apoptosis was detected by flow cytometry, and statistics Analysis, ($n = 3$) $^*P < 0.05$. Transfect miR-5100 minic or miR-5100 minic NC (control group) into AGS cells. (E-F): Western blot was used to detect the expression of caspase3 and cleaved-caspase3 protein, and statistical analysis was performed on cleaved-caspase3 protein, $^*P < 0.05$; (G-H): Apoptosis was measured by flow cytometry and the apoptotic rate Statistical analysis was performed ($n = 3$), $^*P < 0.05$. Transfect miR-5100 inhibitor or miR-5100 inhibitor NC (control group) into MGC80-3 cells. (I-J): LC3B protein expression was detected by western blot, and the ratio of LC3BII/LC3BI was statistically analyzed ($n = 3$), $^*P < 0.05$; (K): Cell autophagy was detected using an autophagosome detection kit. Transfect miR-5100 minic or miR-5100 minic NC (control group) into AGS cells. (L-M): LC3B protein expression was detected by western blot, LC3BI and LC3BII proteins were quantified, and the ratio of LC3BII/LC3BI was statistically analyzed ($n = 3$), $^*P < 0.05$; N: cells were detected using an autophagosome detection kit Autophagy.

microscopy (Fig. 1N). In summary, we conclude that miR-5100 can promote gastric cancer cell apoptosis and inhibit gastric cancer cell autophagy

CAAP1 inhibits apoptosis and promotes autophagy in gastric cancer cells

We found that CAAP1 was expressed at a low level in the MGC80-3 cell line and highly expressed in the AGS cell line (Fig. S2A, S2B). To investigate whether CAAP1 has an effect on the apoptosis and autophagy of gastric cancer cells, the CAAP1 expression plasmid or control plasmid was transfected into the MGC80-3 cell line. Western blot detected a decrease in Cleaved-Caspase3 protein expression ($P < 0.05$) (Fig. 2A, B), and flow cytometry detected a decrease in apoptosis levels ($P < 0.05$) (Fig. 2C, D). The expression of Cleaved-Caspase3 protein increased after transfection of si-CAAP1 in AGS cell lines ($P < 0.05$) (Fig. 2E, 2), and the level of apoptosis increased ($P < 0.05$) (Fig. 2G, H). Next, our experimental results found that CAAP1 promoted the protein ratio of LC3BII/I in MGC80-3 cells ($P < 0.05$) (Fig. 2I, J), and promoted autophagy in MGC80-3 cells (Fig. 2K). After transfection of si-CAAP1 in AGS cells, the protein ratio of LC3BII/I was detected to decrease ($P < 0.05$) (Fig. 2L, M), and the autophagosome content decreased (Fig. 2N). The above experimental results indicate that CAAP1 may inhibit the apoptosis of gastric cancer cell lines and promote autophagy.

miR-5100 inhibits CAAP1 protein expression by targeting CAAP1 3′ UTR

The above studies indicate that miR-5100 can promote apoptosis and inhibit autophagy in gastric cancer cells. At the same time, we also found that CAAP1 can inhibit apoptosis and promote autophagy in gastric cancer cells. The TargetScanHuman (http://www.targetscan.org/vert_72/) website was used to analyze the CAAP1 3′UTR sequence. The analysis results showed that there were three binding sites between CAAP1′s 3′UTR and miR-5100 (Fig. 3A). Next, we constructed the CAAP1 3′UTR luciferase reporter plasmid (Fig. 3B). When the miR-5100 minic or minic control was co-transfected with the CAAP1 3′UTR luciferase reporter plasmid or mutant plasmid, it was co-transfected with the control group. In contrast, miR-5100 minic can inhibit the luciferase activity of the CAAP1 3′UTR luciferase reporter plasmid, but miR-5100 minic has no effect on the fluorescent activity of the CAAP1 3′UTR mutant luciferase reporter plasmid ($P < 0.01$) (Fig. 3C). To further verify that miR-5100 can participate in CAAP1 protein expression, miR-5100 minic or miR-5100 minic NC was transfected into AGS cells, and miR-5100 inhibitor or miR-5100 inhibitor NC was transfected into MGC80-3 cells The expression of CAAP1 protein was detected by blotting. The results showed that miR-5100 minic could inhibit the expression of CAAP1 protein, while miR-5100 inhibitors could promote the expression of CAAP1

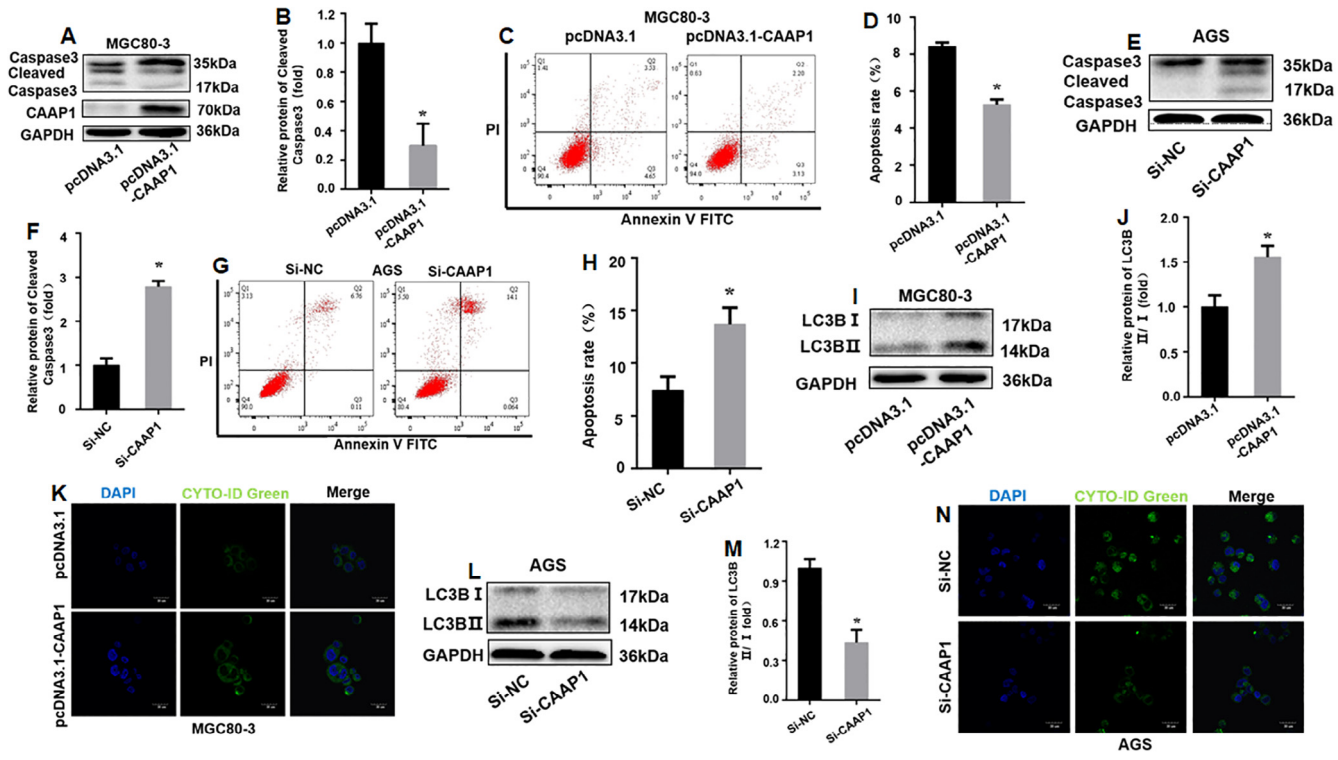

Fig. 2. CAAP1 inhibits apoptosis and promotes autophagy in gastric cancer cells. Transfect CAAP1 expression plasmid or empty vector (control group) into MGC8-3 cells. (A-B): caspase3 and cleaved-caspase3 protein expressions were detected by western blot, and cleaved-caspase3 protein was statistically analyzed ($n = 3$), $^*P < 0.05$; (C-D): Cell dysfunction was detected by flow cytometry Death, and statistical analysis of cell apoptosis rate ($n = 3$), $^*P < 0.05$. Transfect si-CAAP1 or si-CAAP1 (control group) into AGS cells. (E-F): caspase3 and cleaved-caspase3 protein expressions were detected by western blot, and cleaved-caspase3 protein was statistically analyzed ($n = 3$), $^*P < 0.05$; (G-H): Cell dysfunction was detected by flow cytometry Death, and statistical analysis of cell apoptosis rate ($n = 3$), $^*P < 0.05$. Transfect CAAP1 or empty vector (control group) into MGC80-3 cells. (I-J): LC3B protein expression was detected by western blot, and the ratio of LC3BII/LC3BI was statistically analyzed ($n = 3$), $^*P < 0.05$; (K): Cell autophagy was detected using an autophagosome detection kit. Transfect si-CAAP1 or si-CAAP1 control (control group) into AGS cells. (L-M): LC3B protein expression was detected by western blot, LC3BI and LC3BII proteins were quantified, and the ratio of LC3BII/LC3BI was statistically analyzed ($n = 3$), $^*P < 0.05$; N: cells were detected using an autophagosome detection kit.

($P < 0.05$) (Fig. 3D, E). In addition, we applied the biotin-avidin pull-down system to test whether miR-5100 can pull down CAAP1. Cardiomyocytes were transfected with biotinylated miR-5100 and harvested for biotin-based pull-down analysis. Real-time RT-PCR analysis revealed that miR-5100 pulls down CAAP1, but the introduction of mutations that disrupt base pairing between CAAP1 and miR-5100 results in miR-5100 being unable to pull down CAAP1, indicating that miR-5100 recognizes CAAP1 with sequence specificity Mode ($P < 0.01$) (Fig. 3F, H). We also used biotin-labeled specific CAAP1 probes and used a reverse pulldown assay to test whether CAAP1 can pull down miR-5100. By Northern blot analysis, miR-5100 was precipitated (Fig. 3G). In summary, CAAP1 seems to be able to directly bind to miR-5100.

MKL1 targets miR-5100 to inhibit gastric cancer cell apoptosis and promote autophagy

We found that MKL-1 was expressed at a higher level in the MGC80-3 cell line and lower in the AGS cell line (Fig. S3A, S3B). In order to investigate whether MKL-1 has an effect on the apoptosis and autophagy of gastric cancer cells, pcDNA-MKL1 plasmid or empty vector (as a negative control) was transfected into AGS cell lines, and western blot results showed that the expression level of Cleaved-Caspase3 protein was reduced ($P < 0.05$) (Fig. 4A, B), the ratio of protein LC3BII/I increased ($P < 0.05$) (Fig. 4C, D), and the results of flow cytometry showed that the level of apoptosis was decreased ($P < 0.05$) (Fig. 4E, F). Subsequently, si-MKL1 or si-NC (negative control) was transfected into MGC80-3 cells. Western blot results showed that the expression level of Cleaved-Caspase3 protein was increased ($P < 0.05$) (Fig. 4G, H), and the protein LC3BII/The I ratio decreased ($P < 0.05$) (Fig. 4I, J), and the results of flow cytometry showed that the apoptosis level increased ($P < 0.05$) (Fig. 4K, L).

Next, we further analyzed the miR-5100 promoter sequence, and found a CArG box (CC (A/T) 6GG box) at −548 to −538 of the miR-5100 promoter, which is the binding site of MKL1 A luciferase reporter plasmid containing the miR-5100 promoter was constructed (Fig. S4A). The pcDNA-MKL1 plasmid or empty vector was co-transfected with the WT-pGL3-miR-5100 plasmid or mutant plasmid. The results of the luciferase report experiment showed that MKL-1 can promote the activity of lucifer plum in the miR-5100 promoter. The miR-5100 promoter mutant plasmid had no effect on luciferase activity ($P < 0.01$) (Fig. S4B). RT-PCR results showed that when MKL1 was over-expressed, the expression level of miR-5100 increased ($P < 0.01$) (Fig. S4C). ChIP analysis was then performed in AGS cells transfected with miR-5100 or minic. Cross-linked chromatin was immunoprecipitated with specific anti-myc-MKL1 antibody or IgG (as a negative control). The precipitated chromatin DNA was then purified and amplified by specific primers across the CArG box in the miR-5100 promoter. The control group was less enriched with IgG and MKL1, and MKL1

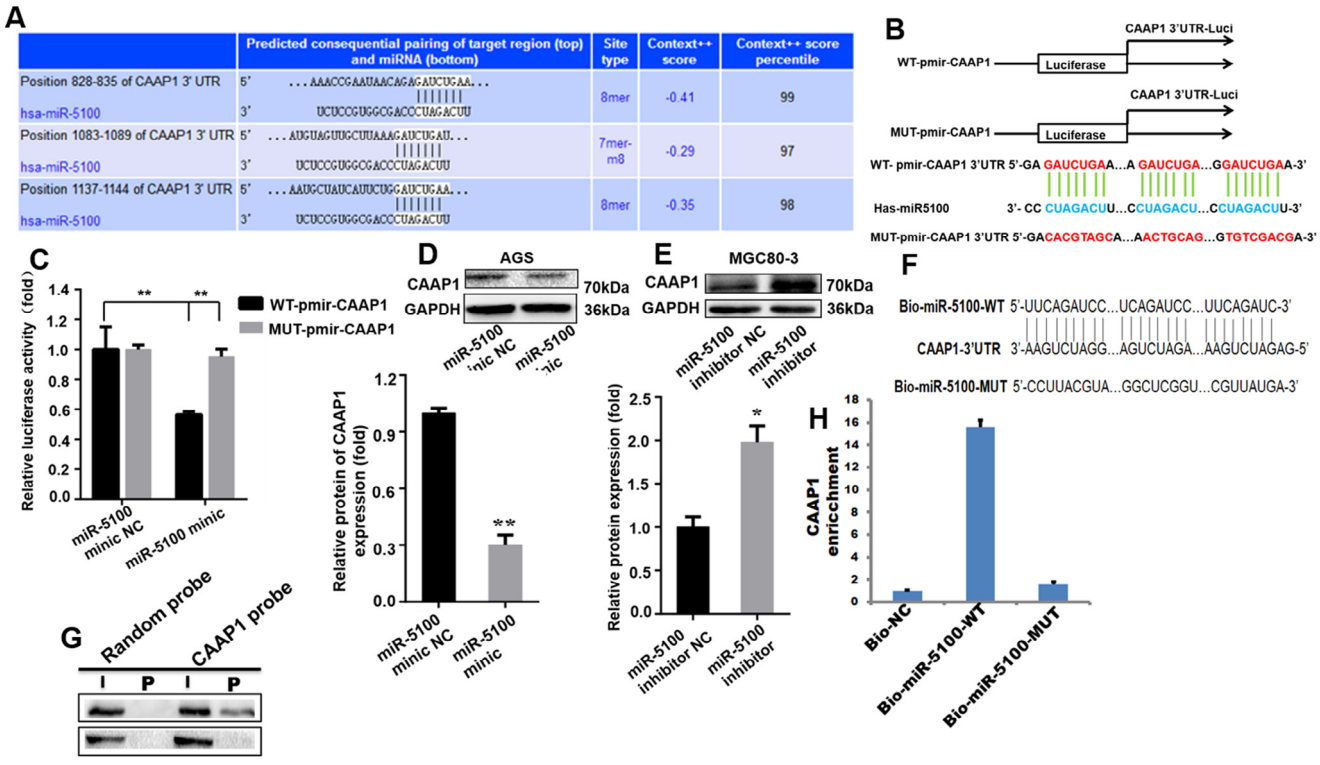

Fig. 3. miR-5100 inhibits CAAP1 protein expression by targeting CAAP1 3′UTR. A: Analysis of the TargetScanHuman (http://www.targetscan.org/vert_72/) website shows that miR-5100 can target the 3′UTR of CAAP1. B: miR-5100 targets the base sequence and mutant sequence of CAAP1 3′UTR. C: miR-5100 minic or miR-5100 minic NC (control group) and WT-pmir-CAAP1 or MUT-pmir-CAAP1 were co-transfected into MGC80-3 cells. The luciferase reporter assay was used to detect whether miR-5100 targeted to bind to CAAP1 3′UTR ($n = 3$); $^{*}P < 0.05$, $^{**}P < 0.01$. D: miR-5100 minic or miR-5100 minic NC (control group) was transfected into AGSA cells, and CAAP1 protein expression was detected by Western blot ($n = 3$), $^{*}P < 0.05$. E: miR-5100 inhibitor or miR-5100 inhibitor NC (control group) was transfected into MGC80-3 cells, and CAAP1 protein expression was detected by western blot ($n = 3$), $^{*}P < 0.05$. F: MUT format of WT and miR-5100 sequences are shown. G: miR-5100 was pulled down by a CAAP1 probe or a random probe. MiR-5100 levels were analyzed by Northern blot. I indicates input (10% of sample is loaded); and P, precipitation (100% of sample is loaded). H: Cardiomyocytes were transfected with biotinylated WT-miR-5100 (Bio-mir-5100-WT) or a biotinylated mutant miR-5100 (Bio-mir-5100-MUT). Biotinylated microRNA that is not complementary to CAAP1 was used as a negative control (Bio-NC). CAAP1 expression level was analyzed by real-time RT-PCR, $^{*}P < 0.05$.

could bind to the CArG box of the miR-5100 promoter ($P < 0.01$) (Fig. S4D). These data indicate that MKL1 can indeed bind to the miR-5100 promoter to promote expression, thereby further affecting the apoptosis and autophagy of gastric cancer cells.

MKL1 targets the promoter of CAAP1 to promote the expression of CAAP1 protein

In order to further explore the molecular mechanism by which MKL1 inhibits gastric cancer cell apoptosis and promotes autophagy, we analyzed the CAAP1 promoter sequence and found that the CArG box exists at −391 bp to −382 bp. Next, we constructed the CAAP1 promoter luciferin Enzyme reporter plasmid (Fig. 5A), pc-DNA-MKL1 or empty vector and CAAP1 promoter luciferase reporter plasmid or mutant plasmid were co-transfected into MGC80-3 cells. The results of luciferase reporter experiments showed that MKL-1 can promote CAAP1 promoter luciferase activity. PC-DNA-MKL1 or pc-DNA (as a control group) (Fig. 5B). RT-QPCR and Western blot experiments in transfected AGS cell lines showed that MKL1 can promote CAAP1 transcription and CAAP1 protein expression ($P < 0.01$) (Fig. 5C–E). To further determine the specific binding of MKL1 to the CAAP1 promoter, ChIP analysis was performed in MGC80-3 cells transfected with MKL1 or vector. Cross-linked chromatin was immunoprecipitated with a specific anti-MKL1 antibody or no antibody (as a negative control). The precipitated chromatin DNA was then purified and amplified by PCR using specific primers that span the CArG box in the CAAP1 promoter. Control (IgG) and negative control (No Ab), PCR produced weak signals. MKL1 can bind to the CArG box of the CAAP1 promoter ($P < 0.01$) (Fig. 5F). These data indicate that MKL1 can bind to the CAAP1 promoter and promote CAAP1 expression, inhibit gastric cancer cell apoptosis and promote autophagy.

In our research, we found that miR-5100 can promote the apoptosis of gastric cancer cells by inhibiting the 3′UTR of CAAP1 and inhibit autophagy, while MKL1 can target the CAAP1 promoter to inhibit the apoptosis of gastric cancer cells and promote autologous bite. Interestingly, we also found the CArG box on the miR-5100 promoter and demonstrated that MKL1 can promote the expression of miR-5100. These data suggest that MKL1/miR-5100/CAAP1 can act as a feedback regulator to influence the apoptosis and autophagy of gastric cancer cells.

To validate our hypothesis, MKL1 and miR-5100 inhibitors or miR-5100 inhibitor NC (as a control) were transfected into AGS cell lines. When MKL1 and miR-5100 inhibitors were co-transformed, Western blot results showed that the expression of CAAP1 protein was higher than that of the control group, the protein ratio of LC3BII/I increased ($P < 0.05$) (Fig. S5A and S5B), and Cleaved-Caspase3 decreased ($P < 0.05$) (Fig. S5C and S5D). The results of flow cytometry experiments showed that the level of apoptosis was decreased ($P < 0.05$) (Fig. S5E, S5F). Cell autophagy was found to increase under the confocal microscope

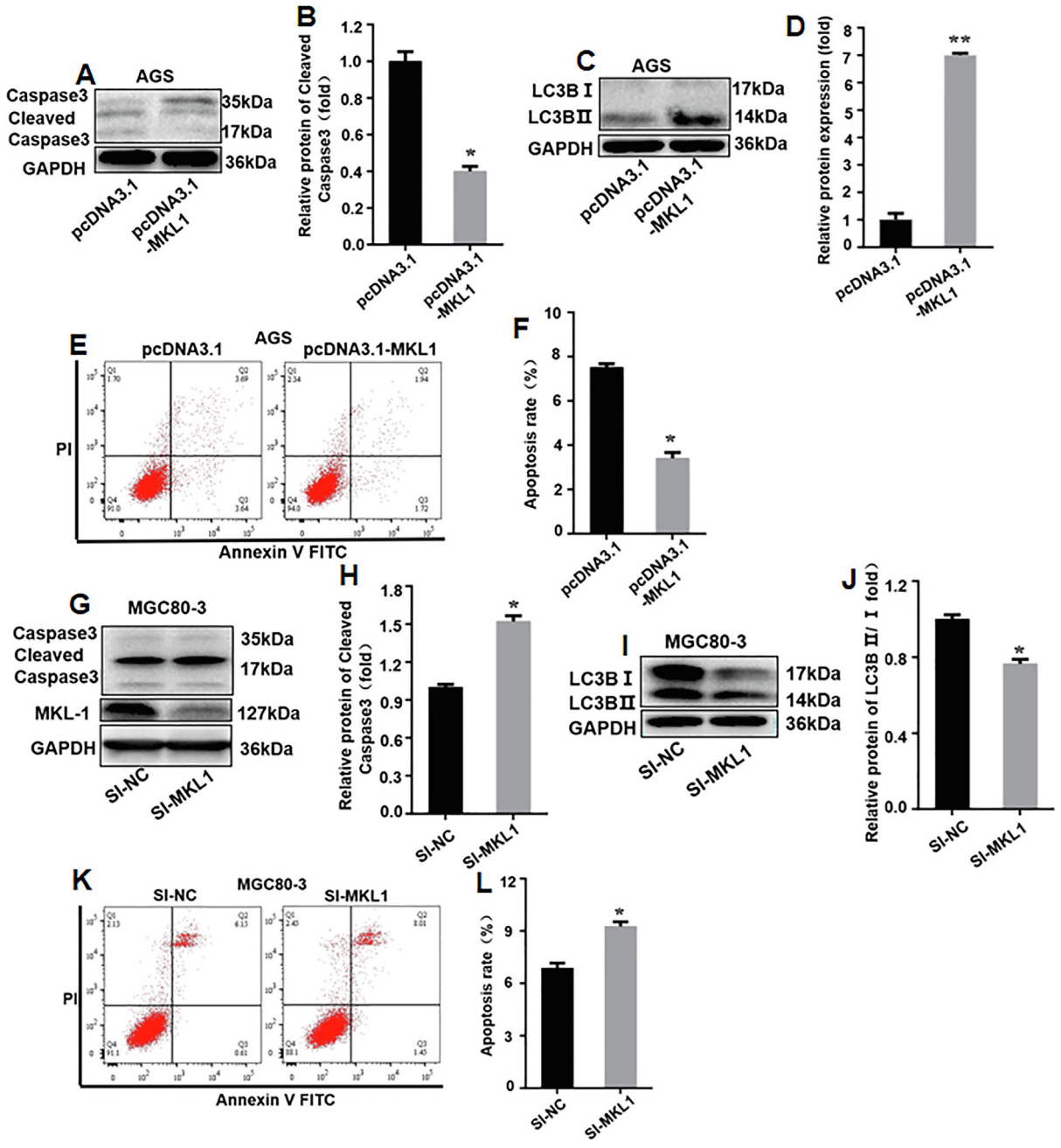

Fig. 4. MKL1 targets miR-5100 to inhibit gastric cancer cell apoptosis and promote autophagy. Transfect MKL1 or empty vector (control group) into AGS cells. (A-B): The expression of caspase3 and cleaved-caspase3 protein was detected by western blot, and the cleaved-caspase3 protein was statistically analyzed ($n = 3$), $^*P < 0.05$. (C-D): Detection of LC3B protein expression by western blot, quantification of LC3BI and LC3BII protein, and statistical analysis of the ratio of LC3BII / LC3BI ($n = 3$), $^*P < 0.05$; (E-F): Detection of cell decay by flow cytometry Death, and statistical analysis of cell apoptosis rate ($n = 3$), $^*P < 0.05$. Transfect si-MKL1 or si-MKL1 NC (control group) into MGC80-3 cells. (G-H): The caspase3 and cleaved-caspase3 protein expressions were detected by western blot, and the cleaved-caspase3 protein was statistically analyzed ($n = 3$), $^*P < 0.05$; (I-J): The LC3B protein expression was detected by western blot. LC3BI and LC3BII protein were quantified, and the ratio of LC3BII/LC3BI was statistically analyzed ($n = 3$), $^*P < 0.05$; (K-L): Apoptosis was detected by flow cytometry, and the apoptosis rate was statistically analyzed ($n = 3$), $^*P < 0.05$.

($P < 0.05$) (Fig. S5G). These data indicate that the MKL1/miR-5100/CAAP1 axis does exist in gastric cancer cells and regulates the apoptosis and autophagy of gastric cancer cells (Fig. S6).

miR-5100 inhibits tumorigenesis in nude mice

In order to study the effect of miR-5100 on gastric cancer cell apoptosis and autophagy in vivo, we constructed an AGS cell line (miR-5100-plko.1) that stably overexpresses miR-5100. 5100-plko.1 cell line and control cell line (plko.1) were injected into nude mice, respectively (Fig. 6A). Compared with the plko.1 group, the tumor formation volume and weight of the miR-5100-plko.1 group were smaller than the control group ($P < 0.01$) (Fig. 6B–D). After 28 days, we observed that miR-5100-plko.1 combined with miR-5100-plko.1+Taxol group had the best tumor healing effect. Next, we performed HE staining (Fig. 6E) and immunohistochemical experiments (Fig. 6F) on the tumor tissue sections. Compared with

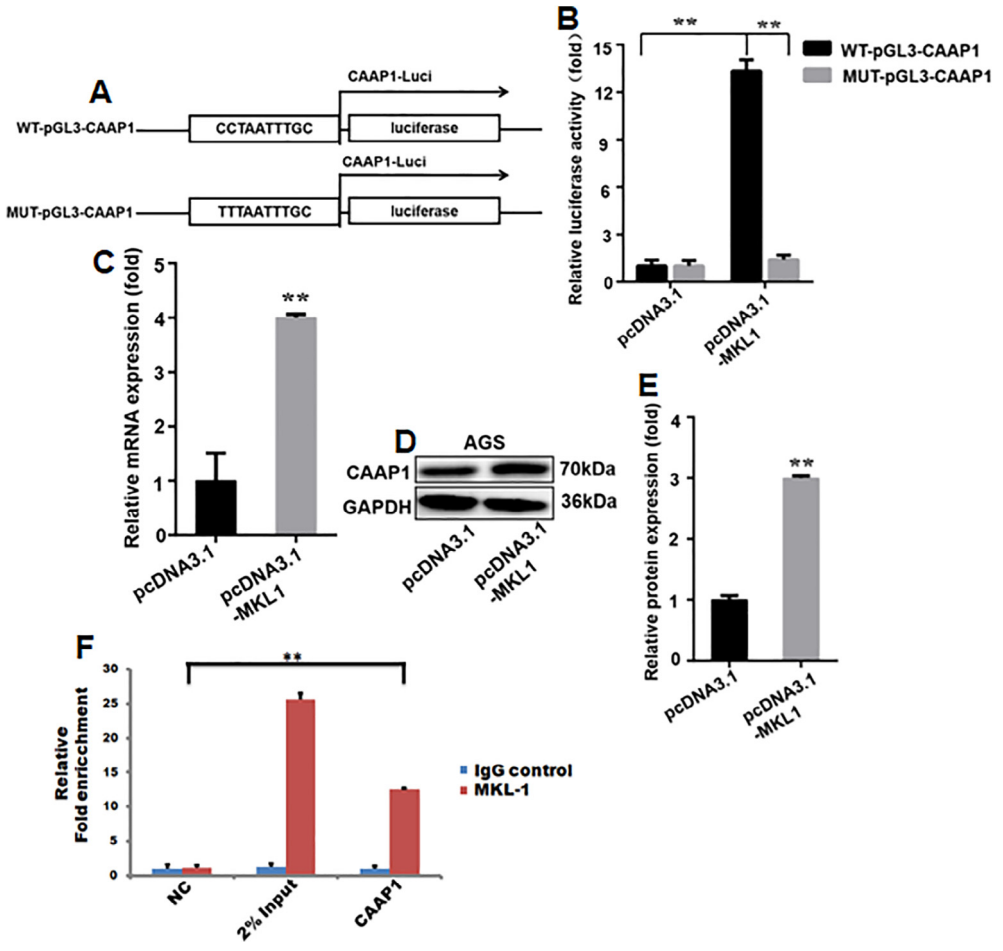

Fig. 5. MKL1 targets the promoter of CAAP1 to promote the expression of CAAP1 protein. A: The base sequence of the CArG box of the wild type (WT-pGL3-CAAP1) and mutant (MUT-pGL3-CAAP1) on the CAAP1 promoter. B: MKL1 or empty vector (control group) was co-transfected with WT-pGL3-CAAP1 or MUT-pGL3-CAAP1 into MGC80-3 cells. The luciferase reporter gene test is used to detect whether MKL1 can target the CAAP1 promoter, $^{*}P < 0.05$, $^{**}P < 0.01$. Transfect MKL1 or empty vector (control group) into AGS cells, (C-E): CAAP1 mRNA expression level was detected by RT-QPCR ($n = 3$) $^{**}P < 0.01$, and CAAP1 protein expression level was detected by western blot, CAAP1 protein was quantitatively and statistically analyzed ($n = 3$), $^{**}P < 0.01$. F: Co-transfect MKL1 or empty vector (control group) with WT-pGL3-miR-5100 or MUT-pGL3-miR-5100 into AGS cells and target CAAP1 according to the method described in ``Experiment'' The ChIP analysis of the primers by PCR showed the amount of DNA in each sample (2% of the input) in the second lane. Immunoprecipitation without primary antibody (No Ab) was used as a mock control, and IgG was used as a negative control.

the control group, the expression level of CAAP1 protein in the tumor tissue of nude mice was higher than that in the experimental group, miR-5100- The CAAP1 protein level was the lowest in the plko.1+Taxol group. Western blot detection of tumor tissue proteins from four groups of nude mice. The results showed that the expression of Cleaved-Caspase3 protein was increased in the tumor tissue of nude mice of group miR-5100-plko.1, while the level of LC3B protein was down-regulated (Fig. 6G). The expression of Cleaved-Caspase3 protein in -5100-plko.1 +Taxol group was higher than that in plko.1+Taxol group, and LC3B protein expression level was down-regulated (Fig. 6H). In summary, we conclude that miR-5100 can promote the apoptosis of gastric cancer cells and inhibit autophagy in vivo and in vitro.

Discussion

Gastric cancer is one of the most common malignant tumors of the digestive tract, but there is no effective method for early disease diagnosis. At present, the treatment of gastric cancer is mainly surgical resection and chemotherapy [22–24]. Surgical removal can effectively remove tumors, but also has some disadvantages, such as large trauma and slow recovery. Moreover, due to the lack of targeted therapies, these traditional chemicals can also cause damage to normal tissues and cells, with more serious toxic side effects [25]. Therefore, studying the etiology and development mechanism of gastric cancer at the molecular level, and developing targeted drug proteins and signaling pathways specifically targeting tumor targets have become the focus of current research [26,27]. The role of microRNAs in GC has been widely studied, and misregulation of miRNAs leads to canceration. Therefore, the abnormal expression of miRNA in GC may be related to the occurrence of disease [28,29].

Current research on miR-5100 is mainly focused on lung cancer and pancreatic cancer. miR-5100 has been reported to promote osteoblast differentiation [30]. In addition, miR-5100 is known to promote tumor growth of lung cancer by promoting G1-S transition and targeting Rab6 [10]. Lawei Yang et al. demonstrated that miR-5100 promotes stem cell-like state of lung cancer cells by regulating Rab6 and mediates lung cancer stem cell resistance to cisplatin [31]. The above literature seems to indicate that miR-5100 may have the ability to inhibit the occurrence

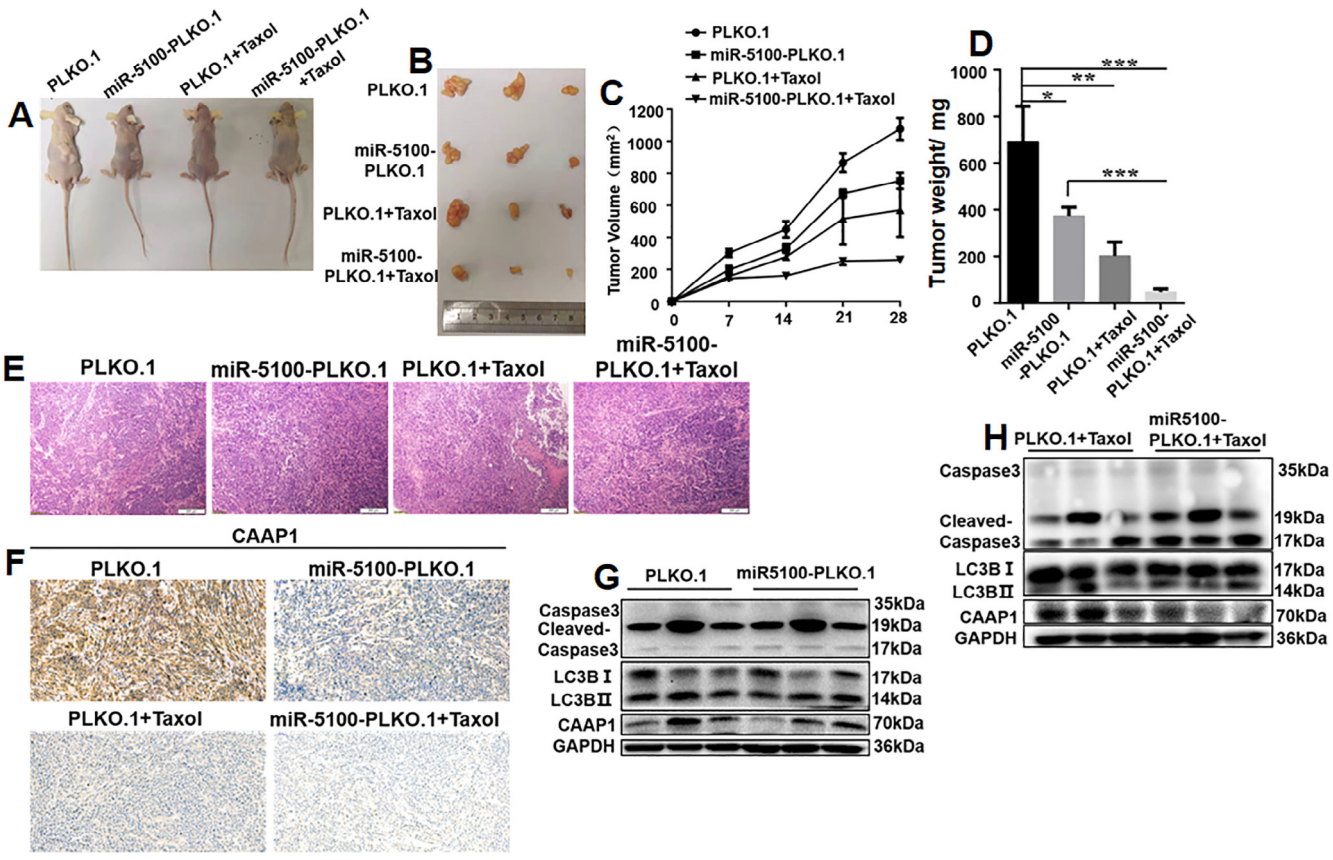

Fig. 6. miR-5100 inhibits tumorigenesis in nude mice. A: Nude mice injected with two different MGC80-3 cell lines or gavage with paclitaxel after 28 days. The images shown represent results for 3 mice. B: Image shows tumor tissue isolated from nude mice with three mice in each group. C: Tumor growth curves of nude mice injected with two different MGC80-3 cell lines or administered paclitaxel after 28 days, and the tumor volume was estimated using calipers; $^{*}P < 0.05$. D: The image shows the statistics of the weight of tumor tissue isolated from nude mice; the weight of the tumor tissue is measured with a balance; $^{*}P < 0.05$. E: Representative H&E-stained sections of the tumor tissues isolated from mice. F: Immunohistochemical analysis of tumor tissue isolated from nude mice, the image shows the results of in-situ analysis of CAAP1 protein. G: Tumor tissues of miR-5100-plko.1 and plko.1 (control group) isolated from nude mice were analyzed for protein expression levels of CAAP1, caspase3, and LC3B by western blot. H: Tumor tissues of miR-5100-plko.1+Taxol group and plko.1+Taxol group (control group) isolated from nude mice were analyzed for protein expression levels of CAAP1, caspase3, and LC3B by western blot.

of cancer, which is different from our findings. Interestingly, in the study of miR-5100 regulating the phenotype of pancreatic cancer cells, Yoshiro Chijiiwa showed that miR-5100 has an inhibitory effect on the occurrence and metastasis of pancreatic cancer [32]. This conclusion is consistent with the findings of this article. There are few reports on miR-5100. The specific effect is still partially controversial in tumor cells. Therefore, further research is needed to clarify the functional difference of miR-5100 in different cancer types.

The latest research shows that CAAP1 is a protein with strong anti-apoptotic ability and has a strong conserved type, which is expressed in various tissues [33]. Research by Yu Zhang et al. Showed that CAAP1 can participate in the apoptosis process of cells. When the CAAP1 gene was knockdown, Research by Yu Zhang et al. Showed that CAAP1 can participate in the apoptosis process of cells. When the CAAP1 gene was knockdown, MCF-7 and A-549 cell lines were proved to be sensitive to apoptosis. And MCF-7 cell line was the most sensitive sensitive. Studies have shown that CAAP interferes with the activation of caspase-10, which in turn regulates the generation of the 11 kDa tBid fragment and caspase-3/9 feedback amplification loop required for effective activation of the mitochondrial death pathway [33]. Qing Yang et al. Found that CAAP1 can regulate cell viability and apoptosis in the study of neonatal brain injury by Long non-coding RNA Snhg3, Studies have shown that the primary hippocampal cells are transfected with si-CAAP1 and treated with hypoxia. Compared with the group, the cell viability was reduced and the apoptotic rate was increased [34]. In this article, we have demonstrated that CAAP1 has anti-apoptotic ability at the protein level in the MGC80-3 cell line and AGS cell line, respectively. At the cell level, the apoptosis level of cells decreases when CAAP1 is overexpressed, and apoptosis levels were increased when CAAP1 was silenced, and these experimental data are consistent with literature reports [12]. It has been documented that most of cell apoptosis is related to autophagy, and the excessive proliferation of tumor cells is often related to cell apoptosis and autophagy imbalance [35–37]. In the study of microRNA-378 on skeleton muscle autophagy and apoptosis, Yan Lia et al. demonstrated that miR-378 can promote cell autophagy while targeting caspase9 to inhibit the occurrence of intracellular apoptosis. This is consistent with the results that gastric cancer cells are always accompanied by inhibition of autophagy during apoptosis. At the same time, our in vitro experiments found that miR-5100 can inhibit the tumor growth of gastric cancer cells in vitro. This further proves that miR-5100 can promote the apoptosis of gastric cancer cells and inhibit autophagy.

MKL1 regulates a variety of processes, including myocyte differentiation [38], cardiovascular development [39,40], development and adult brain [41] neuronal network reconstruction, megakaryocyte differentiation

and migration [20,42,43], cell motor function regulation, Epithelial-mesenchymal transition [44–46]. Notably, there is increasing evidence that the myocardin/MKL family is involved in inhibiting cell proliferation and cell cycle progression. myocardin and MKL1 have antiproliferative effects in a variety of cell lines [47–50]. However, there are few reports on whether MKL1 participates in the process of apoptosis. We first discovered that MKL1 can inhibit the apoptosis of gastric cancer cells and promote the occurrence of autophagy in gastric cancer cells.

In our study, MKL1 can target CAAP1 to inhibit the apoptosis of gastric cancer cells and promote the occurrence of autophagy, which seems to mean that MKL1 can be used as a tumor-promoting gene in gastric cancer cells. We also found that miR-5100 can also target CAAP1 to promote the apoptosis of gastric cancer cells and inhibit the occurrence of autophagy, which seems to mean that miR-5100 acts as a tumor suppressor gene in gastric cancer cells. Interestingly, we found that MKL1 can target the miR-5100 promoter and promote the expression of miR-5100, which forms a loop. In other words, when the cells are at a normal level, MKL1/miR-5100/CAAP1 can form a negative feedback regulation, so that the cell obtains autophagy and apoptosis in a normal state to maintain the homeostasis of the cell. When the cell is exposed to external stimuli, this homeostasis will be broken. MKL1 or miR-5100 loses a state of mutual checks and balances, causing the cell's autophagy or apoptosis to become disordered and cancerous.

Conclusion

In summary, our study found that MKL1/miR-5100/CAAP1 forms a circuit in cells to jointly regulate the homeostasis of apoptosis and autophagy of gastric cancer cells. In vitro proved that miR-5100 can inhibit tumor growth of gastric cancer cells Next, we will further explore MKL1/miR-5100/CAAP1 in gastric cancer. How to interact with each other, how to affect the transcription of target genes for gastric cancer apoptosis, how related signaling pathways regulate this regulation and other molecular mechanisms, and finally to clarify the exact molecular mechanism of gastric cancer cell apoptosis and reveal MKL1/miR-5100/CAAP1 interaction provides basic theoretical basis for regulating gastric cancer cell apoptosis and new functional mechanisms during autophagy. It also provides basic support for the treatment and prognostic intervention of gastric cancer and new drug targets.

Acknowledgements

This work was financially supported by National Natural Science Foundation of China (No. 31501149, 31770815, 31570764) and Hubei Natural Science Foundation (2017CFB537) and Educational Commission of Hubei (B2017009). Hubei Province Health and Family Planning Scientific Research Project (WJ2017M173, WJ2019M255) and the Science and Technology Young Training Program of the Wuhan University of Science and Technology (2016xz035, 2017xz027) and the Innovation and Entrepreneurship Fund for Graduate of Wuhan University of Science and Technology (JCX2016024, JCX2017032, JCX2017033).

Appendix A. Supplementary data

Supplementary data to this article can be found online at https://doi.org/10.1016/j.neo.2020.03.001.

References

1. Ma L, Chen X, Li C, et al. miR-129-5p and-3p co-target WWP1 to suppress gastric cancer proliferation and migration. *J Cell Biochem* 2019;7527–38.
2. McGuire S. *World cancer report 2014. Geneva, Switzerland: World Health Organization, international agency for research on cancer, WHO Press, 2015*. Oxford University Press; 2016.
3. Ferlay J, Soerjomataram I, Dikshit R, et al. Cancer incidence and mortality worldwide: sources, methods and major patterns in GLOBOCAN 2012. *Int J Cancer* 2015;**136**:E359–86.
4. Wang T, Hou J, Jian S, et al. miR-29b negatively regulates MMP2 to impact gastric cancer development by suppress gastric cancer cell migration and tumor growth. *J Cancer.* 2018;**9**:3776.
5. Johnson SM, Grosshans H, Shingara J, et al. RAS is regulated by the let-7 microRNA family. *Cell* 2005;**120**:635–47.
6. He L, Thomson JM, Hemann MT, et al. A microRNA polycistron as a potential human oncogene. *Nature* 2005;**435**:828.
7. Xu Z, Li Z, Wang W, et al. MIR-1265 regulates cellular proliferation and apoptosis by targeting calcium binding protein 39 in gastric cancer and thereby, impairing oncogenic autophagy. *Cancer Lett* 2019;**449**:226–36.
8. Zeng Y, Yi R, Cullen BR. MicroRNAs and small interfering RNAs can inhibit mRNA expression by similar mechanisms. *Proc Natl Acad Sci* 2003;**100**:9779–84.
9. HutvÄgner G, Zamore PD. A microRNA in a multiple-turnover RNAi enzyme complex. *Science* 2002;**297**:2056–60.
10. Huang H, Jiang Y, Wang Y, et al. miR-5100 promotes tumor growth in lung cancer by targeting Rab6. *Cancer Lett* 2015;**362**:15–24.
11. Cheng Y, Li Z, Xie J, et al. MiRNA-224-5p inhibits autophagy in breast cancer cells via targeting Smad4. *Biochem Biophys Res Commun* 2018;**506**:793–8.
12. Aslam MA, Alemdehy MF, Pritchard CE, et al. Towards an understanding of C9orf82 protein/CAAP1 function. *PLoS ONE* 2019;**14** e0210526.
13. Cen B, Selvaraj A, Burgess RC, et al. Megakaryoblastic leukemia 1, a potent transcriptional coactivator for serum response factor (SRF), is required for serum induction of SRF target genes. *Mol Cell Biol* 2003;**23**:6597–608.
14. Wang Z, Cheng Y, Abraham JM, et al. RNA sequencing of esophageal adenocarcinomas identifies novel fusion transcripts, including NPC1-MELK, arising from a complex chromosomal rearrangement. *Cancer* 2017;**123**:3916–24
15. AyllÆn V, Vogel-GonzÄlez M, GonzÄlez-Pozas F, et al. New hPSC-based human models to study pediatric Acute Megakaryoblastic Leukemia harboring the fusion oncogene RBM15-MKL1. *Stem Cell Res* 2017;**19**:1–5.
16. Scharenberg MA, Chiquet-Ehrismann R, Asparuhova MB. Megakaryoblastic leukemia protein-1 (MKL1): increasing evidence for an involvement in cancer progression and metastasis. *Int J Biochem Cell Biol* 2010;**42**:1911–4.
17. Xu W, Xu H, Fang M, Wu X, Xu Y. MKL1 links epigenetic activation of MMP2 to ovarian cancer cell migration and invasion. *Biochem Biophys Res Commun* 2017;**487**:500–8.
18. Li JP, Liao XH, Xiang Y, et al. MKL1/miR34a/FOXP3 axis regulates cell proliferation in gastric cancer. *J Cell Biochem* 2019;**120**:7814–24.
19. Kubiniok P, Lavoie H, Therrien M, Thibault P. Time-resolved phosphoproteome analysis of paradoxical RAF activation reveals novel targets of ERK. *Mol Cell Proteomics* 2017;**16**:663–79.
20. Hu X, Liu ZZ, Chen X, et al. MKL1-actin pathway restricts chromatin accessibility and prevents mature pluripotency activation. *Nat Commun* 2019;**10**:1695.
21. Bodelon C, Oh H, Chatterjee N, et al. Association between breast cancer genetic susceptibility variants and terminal duct lobular unit involution of the breast. *Int J Cancer* 2017;**140**:825–32.
22. Roviello G, Ravelli A, Fiaschi AI, et al. Apatinib for the treatment of gastric cancer. *Exp Rev Gastroenterol Hepatol* 2016;**10**:887–92.
23. Yin L, Wang J, Huang F, et al. Inhibitory effect of apatinib on HCT-116 cells and its mechanism. *Nan fang yi ke da xue xue bao= J Southern Med Univ* 2017;**37**:367–72.
24. Tong X-z, Wang F, Liang S, et al. Apatinib (YN968D1) enhances the efficacy of conventional chemotherapeutical drugs in side population cells and ABCB1-overexpressing leukemia cells. *Biochem Pharmacol* 2012;**83**:586–97.
25. Edelman MJ, Wang X, Hodgson L, et al. Phase III randomized, placebo-controlled, double-blind trial of celecoxib in addition to standard chemotherapy for advanced non–small-cell lung cancer with cyclooxygenase-2 overexpression: CALGB 30801 (Alliance). *J Clin Oncol* 2017;**35**:2184.
26. Scagliotti GV, Von Pawel J, Novello S, et al. Phase III multinational, randomized, double-blind, placebo-controlled study of tivantinib (ARQ 197) plus erlotinib versus erlotinib alone in previously treated patients with locally advanced or metastatic nonsquamous non-small-cell lung cancer2015.

27. Ramalingam SS, Shtivelband M, Soo RA, et al. Randomized Phase II study of carboplatin and paclitaxel with either linifanib or placebo for advanced nonsquamous non–small-cell lung cancer. *J Clin Oncol* 2015;**33**:433.
28. Wu W, Lee C, Cho C, et al. MicroRNA dysregulation in gastric cancer: a new player enters the game. *Oncogene* 2010;**29**:5761.
29. Pan H-W, Li S-C, Tsai K-W. MicroRNA dysregulation in gastric cancer. *Curr Pharm Des* 2013;**19**:1273–84.
30. Wang H, Cui Y, Luan J, et al. MiR-5100 promotes osteogenic differentiation by targeting Tob2. *J Bone Miner Metab* 2017;**35**:608–15.
31. Yang L, Lin Z, Wang Y, et al. MiR-5100 increases the cisplatin resistance of the lung cancer stem cells by inhibiting the Rab6. *Mol Carcinog* 2018;**57**:419–28.
32. Chijiiwa Y, Moriyama T, Ohuchida K, et al. Overexpression of microRNA-5100 decreases the aggressive phenotype of pancreatic cancer cells by targeting PODXL. *Int J Oncol* 2016;**48**:1688–700.
33. Zhang Y, Johansson E, Miller ML, et al. Identification of a conserved anti-apoptotic protein that modulates the mitochondrial apoptosis pathway. *PLoS ONE* 2011;**6** e25284.
34. Yang Q, Wu M-F, Zhu L-H, Qiao L-X, Zhao R-B, Xia Z-K. Long non-coding RNA Snhg3 protects against hypoxia/ischemia-induced neonatal brain injury. *Exp Mol Pathol* 2020;**112** 104343.
35. Li Y, Jiang J, Liu W, et al. microRNA-378 promotes autophagy and inhibits apoptosis in skeletal muscle. *Proc Natl Acad Sci* 2018;**115**:E10849–58.
36. Wang J, Chen T, Wang L, et al. MicroRNA-627-5p inhibits the proliferation of hepatocellular carcinoma cells by targeting BCL3 transcription coactivator. *Clin Exp Pharmacol Physiol* 2019.
37. Ramazani M, Jaktaji RP, Shirazi FH, Tavakoli-Ardakani M, Salimi A, Pourahmad J. Analysis of apoptosis related genes in nurses exposed to anti-neoplastic drugs. *BMC Pharmacol Toxicol* 2019;**20**:1–9.
38. Selvaraj A, Prywes R. Megakaryoblastic leukemia-1/2, a transcriptional co-activator of serum response factor, is required for skeletal myogenic differentiation. *J Biol Chem* 2003;**278**:41977–87.
39. Parmacek MS. Myocardin-related transcription factors: critical coactivators regulating cardiovascular development and adaptation. *Circ Res* 2007;**100**:633–44.
40. Cheng X, Xu S, Pan J, et al. MKL1 overexpression predicts poor prognosis in patients with papillary thyroid cancer and promotes nodal metastasis. *J Cell Sci* 2019;**132**:jcs231399.
41. Mokalled MH, Johnson A, Kim Y, Oh J, Olson EN. Myocardin-related transcription factors regulate the Cdk5/Pctaire1 kinase cascade to control neurite outgrowth, neuronal migration and brain development. *Development* 2010;**137**:2365–74.
42. Ly DL, Waheed F, Lodyga M, et al. Hyperosmotic stress regulates the distribution and stability of myocardin-related transcription factor, a key modulator of the cytoskeleton. *Am J Physiol-Cell Physiol* 2012;**304**:C115–27.
43. Cheng E-c, Luo Q, Bruscia EM, et al. Role for MKL1 in megakaryocytic maturation. *Blood* 2009;**113**:2826–34.
44. Smith EC, Teixeira AM, Chen RC, et al. Induction of megakaryocyte differentiation drives nuclear accumulation and transcriptional function of MKL1 via actin polymerization and RhoA activation. *Blood* 2013;**121**:1094–101.
45. Elberg G, Chen L, Elberg D, Chan MD, Logan CJ, Turman MA. MKL1 mediates TGF-β1-induced α-smooth muscle actin expression in human renal epithelial cells. *Am J Physiol-Renal Physiol* 2008;**294**:F1116–28.
46. Mihira H, Suzuki HI, Akatsu Y, et al. TGF-β-induced mesenchymal transition of MS-1 endothelial cells requires Smad-dependent cooperative activation of Rho signals and MRTF-A. *J Biochem* 2011;**151**:145–56.
47. Descot A, Hoffmann R, Shaposhnikov D, Reschke M, Ullrich A, Posern G. Negative regulation of the EGFR-MAPK cascade by actin-MAL-mediated Mig6/Errfi-1 induction. *Mol Cell* 2009;**35**:291–304.
48. Kimura Y, Morita T, Ki Hayashi, Miki T, Sobue K. Myocardin functions as an effective inducer of growth arrest and differentiation in human uterine leiomyosarcoma cells. *Cancer Res* 2010;**70**:501–11.
49. Tang R-H, Zheng X-L, Callis TE, et al. Myocardin inhibits cellular proliferation by inhibiting NF-κB (p65)-dependent cell cycle progression. *Proc Natl Acad Sci* 2008;**105**:3362–7.
50. Zheng P, Yin Z, Wu Y, Xu Y, Luo Y, Zhang T-C. LncRNA HOTAIR promotes cell migration and invasion by regulating MKL1 via inhibition miR206 expression in HeLa cells. *Cell Commun Signal* 2018;**16**:5.